



Effect of surfactant on morphology and pore size of polysulfone membrane

Qian Ge¹ · Lei Ding¹ · Tong Wu¹ · Guan Xu¹ · Feng Yang¹  · Ming Xiang¹

Received: 26 June 2017 / Accepted: 27 November 2017 / Published online: 14 December 2017
© Springer Science+Business Media B.V., part of Springer Nature 2017

Abstract

The skin layer structure can be changed by adjusting the diffusion rate of the non-solvent into the polymer solution between membrane and coagulation bath through adding surfactant into either coagulation bath or dope solution. When adding SDS in coagulation bath, the variation trend of apparent diffusion coefficient during phase separation and scanning electron microscopy morphology of resultant membranes indicated that, at the beginning SDS migrated to the membrane-bath interface during phase separation process, playing a role as mechanical barrier within 0.15 wt% SDS concentration. Once the SDS concentration exceeds CMC, the remaining SDS will form micelles act as a carrier, hence, the phase separation rate accelerated. The membranes were characterized roughness parameters, obtained by the atomic force microscopic technique. While adding surfactant in the dope solution, compared with SDS addition into the coagulation bath, apparent diffusion coefficient and SEM morphology showed the similar trend, and the excellent range of SDS concentration is 0.08 wt%-0.1 wt%. As changing the nature of surfactant in the dope solution, we found that, with the increase of surfactant hydrophile-lipophile balance (HLB) value, the rate of phase separation speeds up, the size of macrovoid increases, flux increases gradually and rejection is weakened.

Keywords Surfactant · Preparation · Polysulfone membranes · Pore size

Introduction

Polysulfone (PSf) membranes are widely used in many applications from electronic film capacitors to gas separation and water purification membrane [1–3]. Phase inversion via

immersion precipitation is a well-known process for preparing Polysulfone (PSf) membranes [4–7]. In the preparation of the membrane, a homogeneous polymer solution containing polymer and adequate solvent is cast on a glass plate and after a short period of solvent evaporation, then immersed in a coagulation bath [8–10]. The diffusive exchange of solvent and non-solvent introduces liquid–liquid phase separation. The phase separated solution leads to a porous, asymmetric structure [11, 12]. The morphology and performance of membranes depend strongly on the thermodynamics as well as kinetics of the phase inversion process [13, 14].

In order to adjust the morphology and performance of membranes, some researchers have changed the concentration of the casting solution and some have changed the coagulation bath temperature [15–18], but the better effective way is to add the surfactant [19–22]. Some researchers immerse the nonwoven fabric scraped with the PSf solution into a coagulation bath containing a certain concentration of sodium dodecyl sulfate (SDS) [23]. This is conducive to the follow-up interface polycondensation reaction, but also beneficial to immerse the aqueous monomer into the polysulfone support layer. The addition of SDS can effectively change the surface tension of the water in the coagulation bath and can change the kinetic

✉ Feng Yang
yangfengscu@126.com

Qian Ge
geqian6859@163.com

Lei Ding
dinglei921022@163.com

Tong Wu
wutong19851128@163.com

Guan Xu
xuguanbs@163.com

Ming Xiang
teylor112@163.com

¹ State Key Laboratory of Polymer Materials Engineering, Polymer Research Institute of Sichuan University, Chengdu 610065, People's Republic of China

process in the phase separation process by some special surface action [24]. So that people can control the coagulation bath SDS content simply to improve the PSf ultrafiltration membrane microstructure, resulting in a more ideal support layer. Alsdeg et al. studied the effect of different content of SDS on the preparation of PES membrane after phase separation [23]. The addition of SDS could significantly alter the membrane surface structure and membrane filtration performance, and the critical micelle concentration (CMC) of SDS in water was the most critical factor.

In addition, the surfactant can also be added as an additive to the casting solution to change the phase separation process [25]. Lin et al. suggested that the affinity of the solvent and the coagulation bath in the casting solution was improved after the addition of the appropriate surfactant, and the phase separation mechanism shifted from the delayed phase separation to the instantaneous phase separation, resulting in the formation of large pores [26, 27]. Bin et al. proposed that the addition of Tween 80 favored the formation of larger pores by interrupting the polymer chain entanglement and improving the miscibility between solvent and coagulant [28]. Sh. Saedi et al. study has demonstrated that the addition of surfactants in the casting solution increases the formation of macrovoids and large finger-like pores in the sub-layer of polysulfone membranes [29]. Most of the research focused on polymer chain and the surfactants interacted at molecular level and polysulfone membrane cross-sectional morphology changes [30–32], while ignoring the diffusion rate of the non-solvent into the polymer solution and the surface morphology. However the diffusion rate has a significant effect on the formation of surface morphology.

The pore size and distribution of the pore structure on the membrane surface affect the process of interfacial polymerization during the preparation of the composite membrane and ultimately affect the filtration performance of the TFC membrane [9, 33–35]. The results show that the integrity of the PA functional layer on the surface of the TFC membrane will be destroyed at these defective structures and irreversibly damage the TFC film when the pore structure on the membrane surface is large [36–38]. In response to this problem, we tried to change the amount of SDS added. Membrane structure was characterized by scanning electron microscopy (SEM), porosity and pore size analysis, and atomic force microscopy (AFM). Membrane performance was evaluated by pure water flux and rejection. On the basis of ensuring the better filtration efficiency of the prepared support layer, the formation of large pore structure is reduced, and the comprehensive performance of the membrane is further improved. On the other hand, the amount of SDS added in the coagulation bath increase the difficulty of post-treatment of SDS in coagulation bath. In order to reduce the dosage of surfactant, the addition of SDS to the casting solution can greatly reduce the dosage of surfactant. Therefore, we added SDS to the casting solution and

selected several other surfactants with large differences in properties as a contrast to study its effect on the phase separation process.

Experimental

Material

Commercial polysulfone (Udel® P-3500, Mn~22 kDa, Solvay.) was used as membrane materials. N,N-dimethylformamide (DMF, Chengdu Kelong Chemical Co., Ltd. purity >99.5%, Analytical reagent) and distilled water were employed in this study as solvent and nonsolvent respectively. Sodium dodecyl sulfate (SDS), sodium dodecyl benzene sulfonate (SDBS), polyoxyethylene sorbitan monolaurate (Tween-20), polyoxyethylene sorbitan monostearate (Tween-80), glycerol monostearate (GMS) and sorbitan monooleate (Span-80) were also purchased from Chengdu Kelong Chemical reagents, analytical grade and were used as surfactants.

Membrane preparation

Phase inversion method was used to prepare asymmetric polysulfone (PSf) membranes. The PSf resin particles were treated in a vacuum oven at 100 °C for 12 h to completely remove the water and then a different composition of the polymer solution (casting solution) was prepared using dry PSf and DMF solvent. PSf was dissolved into the solvent mixture with different additives. The casting solution was evenly coated on the polyester sheet with a scraper, and the film thickness was controlled at 300 μm. The PSf sheet coated with the casting solution was then rapidly immersed in a non-solvent coagulation bath (temperature controlled at 25 °C). Finally, the membrane is removed from the deionized water and dried at room temperature. The humidity of the environment during the preparation of the membrane is about 60%.

Characterization

Phase separation apparent diffusion coefficient test

The phase separation process was observed by optical microscope. At the same time in the phase separation process every 30 s using a digital camera to take pictures immediately. Sample preparation was carried out as described by Matz [39] and a drop (about 30 ul) of the coating solution was placed between the slide and the edge of the coverslip. And then touch the edge of the coverslip with a drop of non-solvent. The non-solvent rapidly enters the gap to contact the edge of the diffused polymer solution. The trend of non-solvent invasion depth was linearly fitted with time. The

apparent diffusion coefficient of the non-solvent of the selected system was calculated.

Membrane pure water flux and rejection rate test

- (1) Test of pure water flux: Moisturizing membrane with appropriate size is under the positive pressure filter flux test. Filtration experiments were carried out using a dead-end filter. The membrane was preloaded for 30 min at a differential pressure of 1.5 bars and then the amount of deionized water through the membrane per unit time was measured at a pressure of 1 bar. Flux is calculated as follows:

$$J = \frac{V}{S \times t} \quad (1)$$

Where J is the measured pure water flux ($L / m^2 \cdot h$), V (L) is the volume of the membrane passing through the area S (m^2) in time t (hour).

- (2) Test of rejection rate: The distilled water at the test flux was replaced with the formulated 1000 ppm PEG 20000 solution, and collected the filtrate when stabilizing. After the filtrate was diluted 100-fold, the concentration of PEG 20000 in the permeated and the stock solution was measured under a visible light spectrophotometer using a dragon doff reagent as a color reagent. Respectively, as C_f and C_p , the rejection rate was:

$$R = \left(1 - \frac{C_p}{C_f}\right) \times 100\% \quad (2)$$

Scanning electron microscopy analysis (SEM)

The prepared hand membrane was freeze-dried with liquid nitrogen to prepare a membrane cross section. The samples were dried and then mounted on an SEM sample rack and coated with gold to prevent charging. The images of the membrane section and the top surface were taken using a Hitachi S-4800 emission scanning electron microscope (FE-SEM).

Atomic force microscopy analysis (AFM)

The roughness of membrane surface was analyzed by an atomic force microscopy (Veeco AFM Dimension 3100). A picture with a scan frequency of 1.3 Hz and a scan size of 1 μm was used for analysis. The surface roughness (R_q), the average roughness (R_a), the peak-to-bottom height (R_z), and the specific surface area of the membrane were used to represent the surface roughness. The specific surface area is the

ratio of the true area of the measured membrane surface to the projection in the vertical direction.

Porosity determination

The porosity of the membrane was represented by calculating the water occupied volume ratio of the membrane when the membrane was in full water state. It is operated by the following steps: The membranes under wet conditions were cut into a certain size of the rectangle. The area is recorded as A (cm^2), the thickness is recorded as h (mm). The surface of the water is wiped with a filter paper and weighed, denoted as W_w (g). The wetted membrane was weighed in an oven at 60 °C and 80 °C for 24 h to ensure complete removal of moisture and a completely dry membrane weighed as W_d (g). The porosity can be calculated using the following formula:

$$P(\%) = \frac{W_w - W_d}{\rho_w \times A \times h} \times 1000 \quad (3)$$

Where P represents the porosity of the calculated sample; ρ_w is the water density, where 1 g / cm^3 are taken. Each sample was done three times in parallel and then calculated as an average.

Compression test

The compression performance of the film was tested using a universal material testing machine (CMT6104, Meters Industrial Systems, Inc.). All samples were dried before testing.

Casting fluid viscosity test

The viscosity of the cast membrane was measured by NDJ-1 rotary viscometer (Shanghai Jingke).

Results and discussion

SDS was added to the coagulation bath

An aqueous solution of different concentrations of SDS was prepared as a coagulation bath of 18 wt% PSf, and the phase separation process was observed under an optical microscope. After the linear fitting, the calculated apparent diffusion coefficient varies with SDS concentration as shown in Fig. 1. Initially, the addition of the surfactant adjusts the surface tension of the casting solution and the coagulation bath to increase the phase separation rate. Then the diffusion rate of the non-solvent into the polymer solution can be reduced with the increase of SDS concentration. At the 0.15 wt% SDS concentration to a minimum, this concentration corresponds

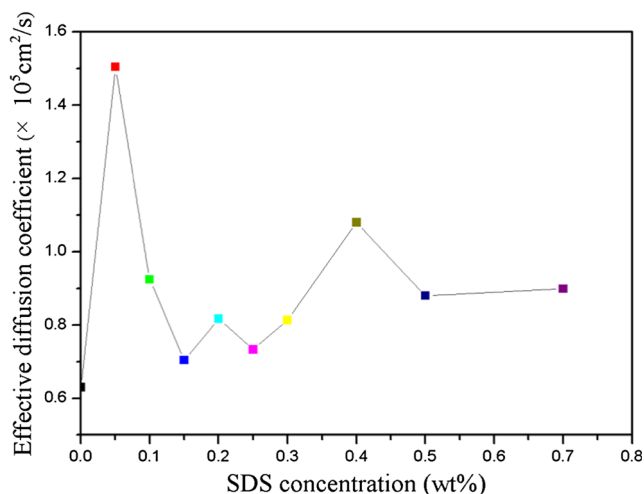


Fig. 1 Influence of SDS concentration in the coagulation bath on the phase separation rate of 18 wt% PSf dope solution

to the critical micelle concentration (CMC). And then, the apparent diffusion coefficient increases progressively with an increase in SDS in the coagulation bath.

Figure 2 shows the cross section and surface SEM of the PSf film prepared by SDS concentration of different coagulation bath. It can be seen that the sample prepared with pure water as the coagulation bath has a smaller thickness. With the increase of SDS concentration, the porosity of the membrane section becomes larger and larger, showing a “floating” state, and a turning point occurs at 0.15 wt% SDS concentrations, and then the macrovoid structure runs through the whole membrane section. The relationship between the phase separation rate and the SDS concentration in the coagulation bath can be explained in the following manner. It is widely accepted that phase separation is a trade-off between thermodynamic enhancement and kinetic hindrance. As the gelled medium is brought into contact with the casting polymer solution, exchange of solvent and non-solvent begins to take place rapidly. When one side of the membrane is in contact with the gelling medium, the solvent casting membrane enters the casting membrane from the inside to the gel medium and the non-solvent moves from the gelation medium into the cast film. Due to the rapid invasion of non-solvent, the proportion of non-solvent in the polymer solution membrane begins to increase. When the ratio of non-solvent increases to a certain value, PSf/DMF/water ternary system begins to become unstable, and the polymer can not be stably present in the system and begins to precipitate. During polymer precipitation, not only is there an exchange of solvent and non-solvent, but also the polymer is constantly moving in solution. The precipitation of polymer initially takes place at the interface to form a skin layer that gradually diffuses into the polymer solution film.

Therefore, the addition of SDS to the coagulation bath can significantly change the tension of the membrane-bath

interface during phase separation, thus influence the mechanism of phase separation, then further affecting the pore structure of the membrane. The concentration of SDS in the presence of macrovoid structure is close to the CMC value. From the surface morphology of the membrane, it can be seen that the size and distribution of surface pores is altered by the addition of SDS in the coagulation bath. With the increase of SDS concentration, the surface pore size decreased first, reached the minimum at 0.15 wt% SDS, and then gradually increased. In contrast to Fig. 1 characterization of the phase separation rate, the addition of SDS in the phase separation process to the membrane bath interface, play a mechanical barrier effect, reducing the phase separation process of solvent and non-solvent exchange process. That is consistent with the mechanism proposed by Alsdeg et al. [23] As shown in Fig. 3 when the concentration of SDS is lower than that of CMC shown in Fig. 3a, with the increase of SDS concentration, the concentration of SDS in the membrane-bath interface is increasing, which gradually hinders the exchange process of DMF and water during phase separation. Leading to the phase separation process being delayed, the formation of the cortex will become thicker and thicker, the surface pores become smaller and smaller. When the SDS concentration exceeds CMC, the dissolved SDS in the coagulation bath will remain at a certain concentration, and the remaining SDS will form micelles. These micelles are very compatible with the solvent DMF, when the phase is separated these micelles act as a carrier for the exudation of DMF in the PSf solution. That in turn accelerates the process of solvent and non-solvent exchange. While, at the beginning of the formation of micelles, micelles are smaller in volume and less in number. With the increase of the concentration of SDS the phase separation rate is gradually increased. As the concentration of SDS increased to a critical value, the size and concentration of micelles tended to be stable. Moreover, the phase separation rate is the balance of thermodynamics and kinetics. Hence, as the phase separation rate is accelerated, the formation of the cortex becomes thinner, and the pore size of the surface pore increases.

The membrane prepared by adding SDS in the coagulation bath was subjected to filtration performance and mechanical properties shown in Fig. 4. The addition of SDS in the coagulation bath decreases the rejection first. With increase the concentration of SDS the rejection increases and reaches the maximum at the CMC, then decreases gradually, indicating that the formation of the cortical pore structure decreases first and then increases. This is consistent with the previous SEM results. The addition of SDS in the coagulation bath can significantly increase the flux of the membrane. With the increase of SDS concentration, the flux decreases first and then increases, and decreases to the minimum at 0.15 wt%. The size of the flux is not only related to the continuity of the membrane cross-section, but also on the porosity of the membrane

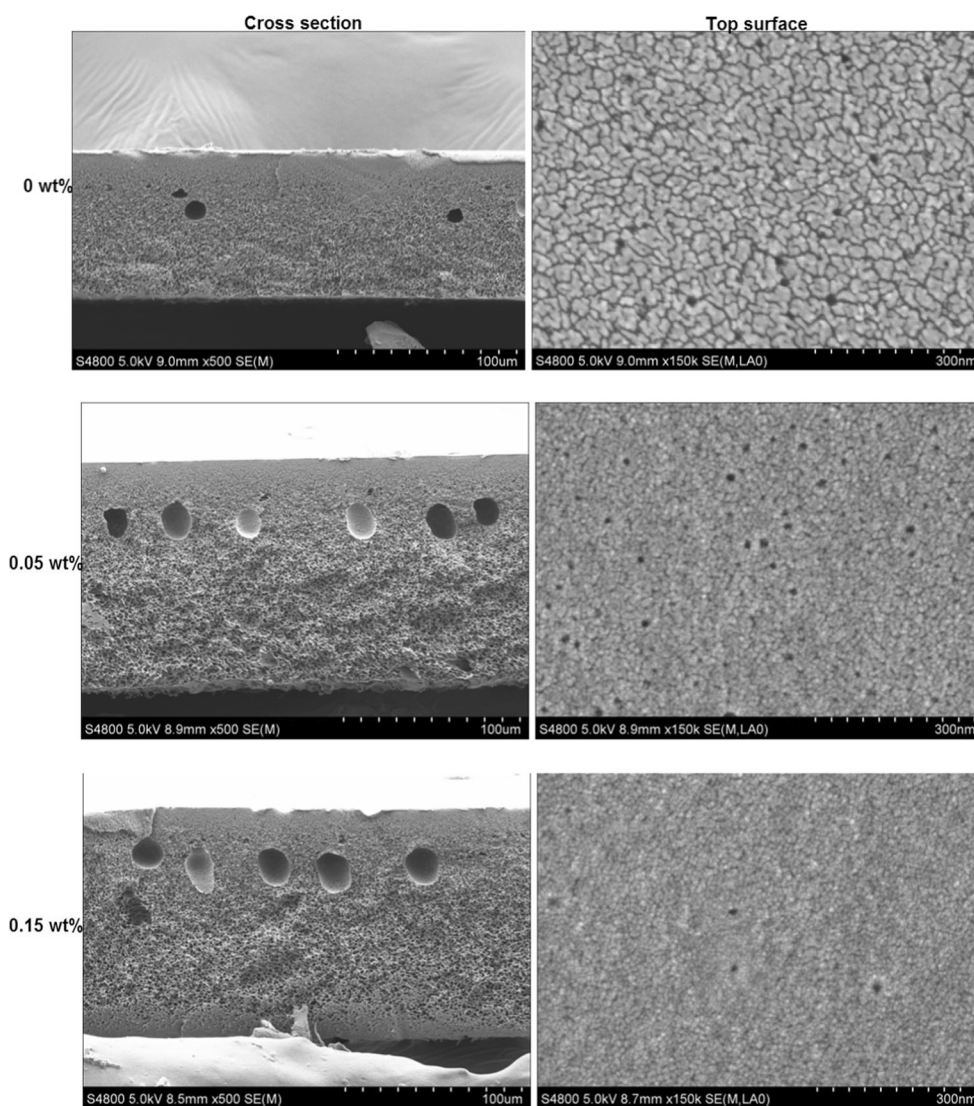


Fig. 2 SEM cross-section and top surface images of membranes prepared from 18 wt% PSf cast dope solutions precipitated in coagulation bath with different SDS concentration

surface. The presence of large pores increases the continuity between the pores of the membrane section, and the membrane surface porosity determines the amount of water that enters the membrane during the test process. Therefore, we believe that, below the CMC, the phase separation rate becomes slower, the membrane cortex thickened, although the pores of the membrane surface become smaller, but there is enough time to induce the formation, resulting in the number will be more, the two contradictory factors together determine the ultimate flux of the membrane. Under 0.15 wt%, with the increase of SDS concentration, the size of the pore structure decreases with the decrease of the porosity of the membrane surface. The increase in the number of pinhole structures contributes to the surface porosity and the flux decreases. In the range of 0.15 wt% -0.25 wt%, the decrease of pore porosity caused by the decrease of pore size is less than the increase of the number of pores to increase the porosity of the membrane

surface, and the flux begins to increase. When the SDS concentration exceeds CMC, the phase separation rate is accelerated. At this point, very low membrane-bath interface tension is also more conducive to solvent-non-solvent exchange. The membrane surface will form a larger pinhole-like structure. The number of which is reduced due to the accelerated rate of phase separation, the porosity of the membrane surface is not changed and the flux tends to be stable. From Fig. 4 (b), it can be seen that the introduction of large pores increases the porosity of the membrane and increases the flux of the membrane to a certain extent, but the compressive capacity of the membrane is decline apparently.

After comprehensive consideration, to make the prepared PSf film pressure resistance is higher, and the filtration efficiency is better (Both retention and flux are maintained at a high level). The concentration of SDS added to the coagulation bath is preferably 0.2–0.25 wt%. At this point, the

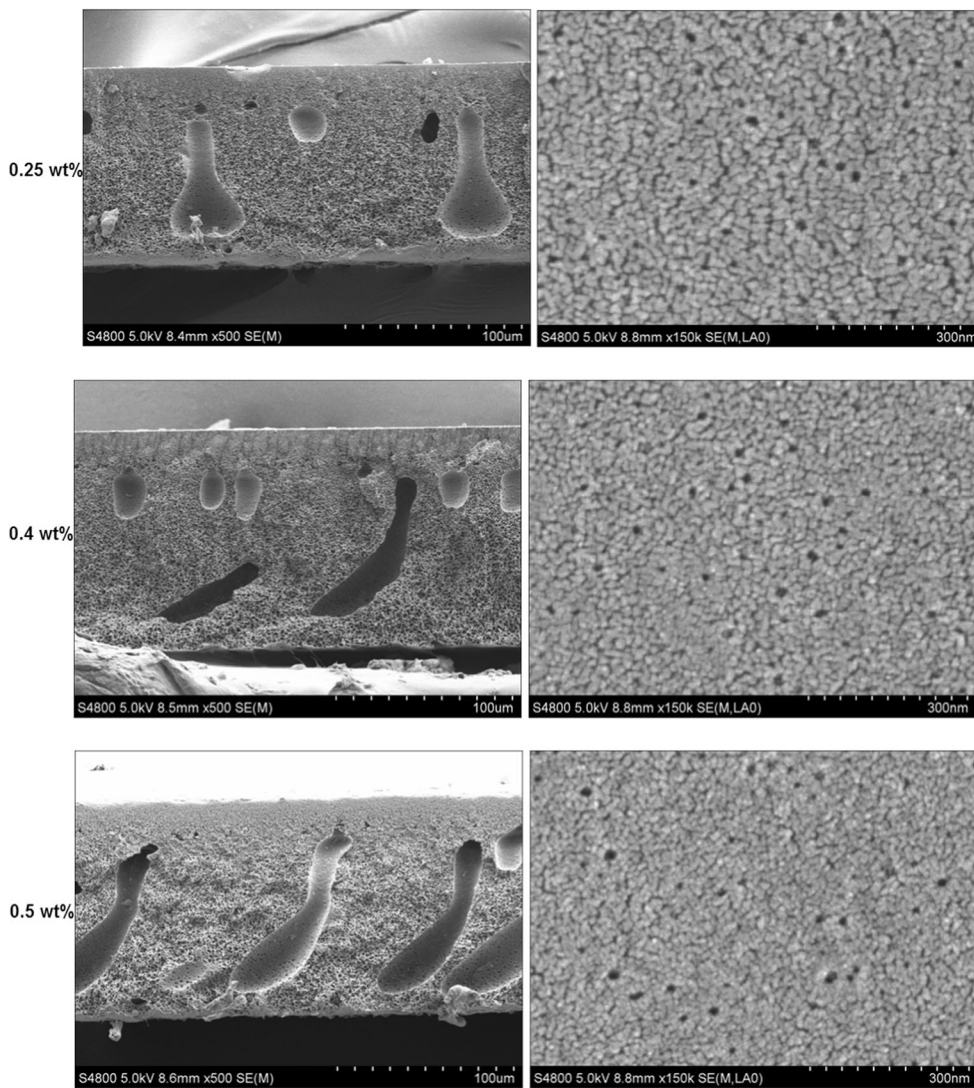


Fig. 2 continued.

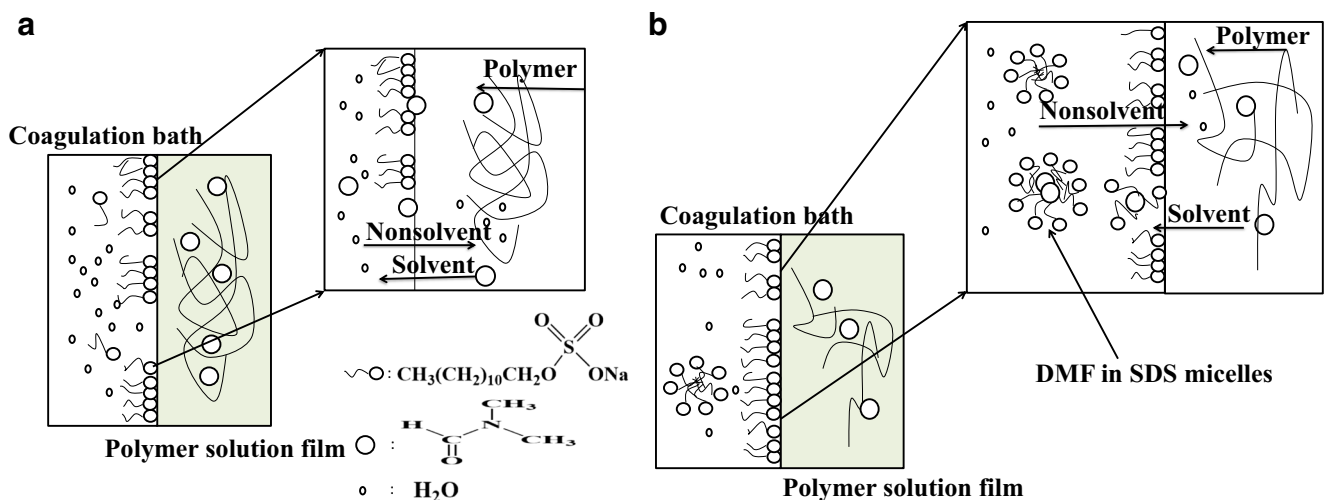


Fig. 3 Schematic drawing of the influence of SDS concentration in coagulation bath on the solvent/non-solvent exchange process at the gelation media/cast polymer solution interface: **a** SDS concentration $< CMC$, and **b** SDS concentration $> CMC$

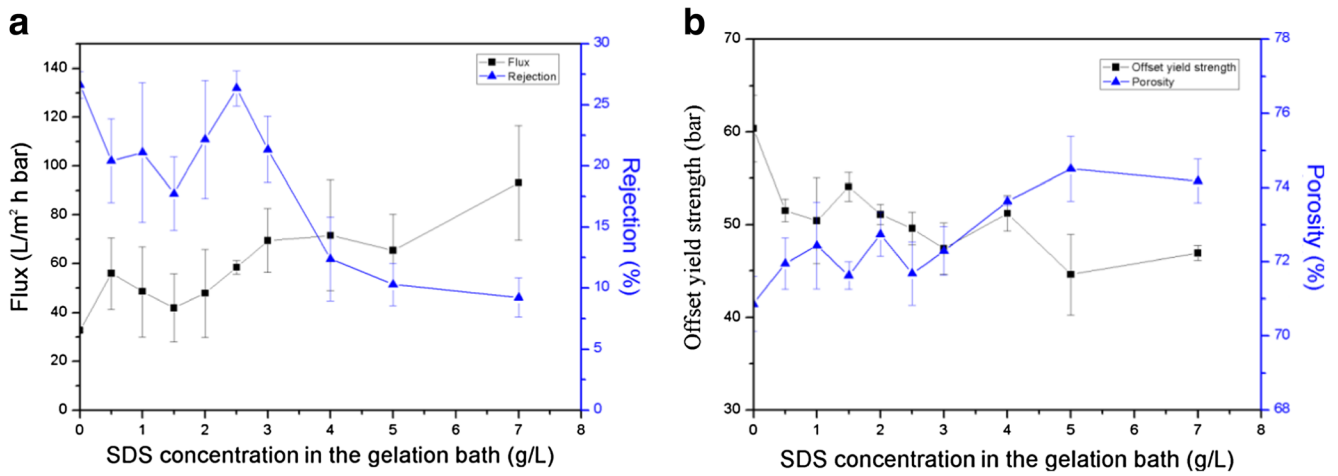


Fig. 4 Flux vs. rejection (a) and off-set yield strength vs. porosity (b) of membranes prepared with 18 wt% PSf cast dope solution precipitated in coagulation bath with different SDS concentration

prepared membrane can withstand about 50 bar of pressure, flux increased by about 50% -100%, while the retention rate can basically maintain the original level.

The relationship between surface morphology and SDS concentration

Usually, the scanning electron microscope image can only see the surface of the membrane surface plan and in the sample preparation when the need for the film spray treatment, the

surface of the film surface will be a certain degree of distortion. Atomic force microscopy (AFM) can more truly reflect the three-dimensional surface of the membrane surface. Thus, in order to characterize the fluctuation of the membrane surface, that is, the surface roughness of the membrane, we conducted an AFM test on the skin cortex. Figure 5 is a three-dimensional map of different SDS contents added to the coagulation bath after the transformation. The addition of SDS significantly changed the morphology of the membrane surface, and the fluctuation structure of the membrane surface

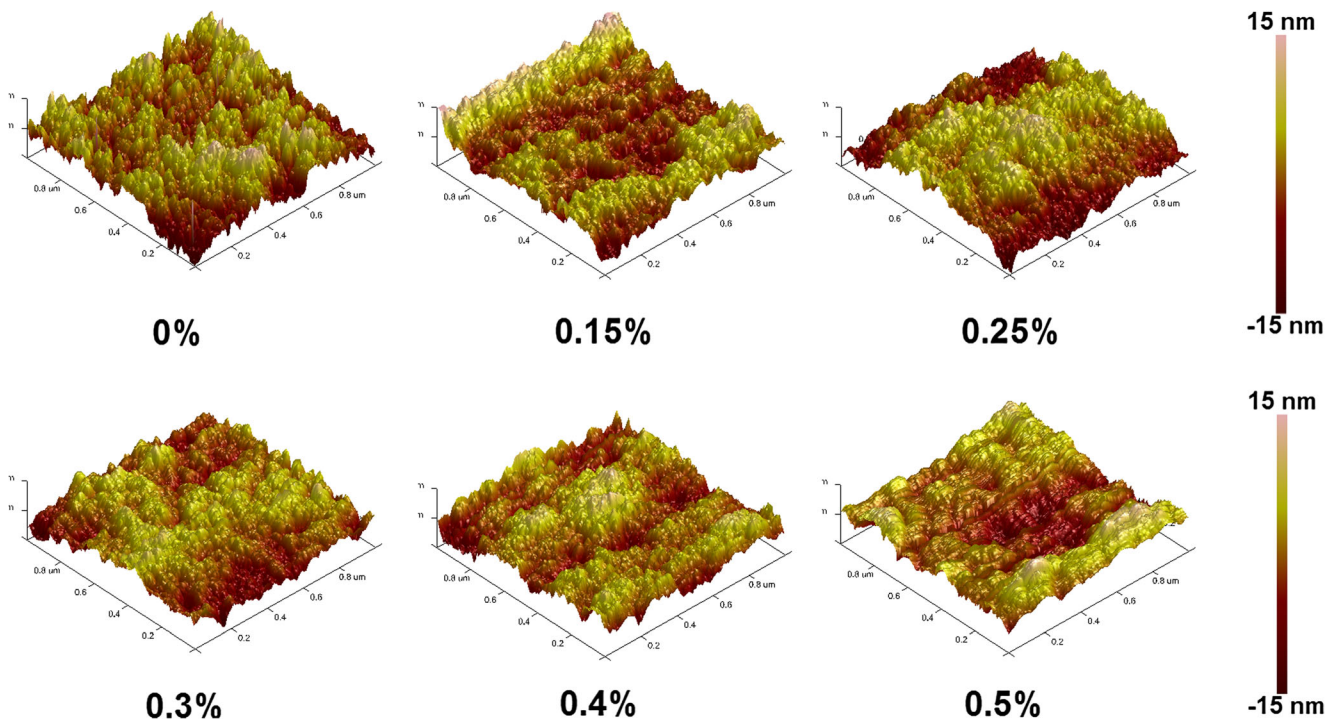


Fig. 5 AFM surface pictures of membranes prepared from 18 wt% PSf cast dope solutions precipitated in coagulation bath with different SDS concentration

Table 1 Roughness parameters and calculated pore parameters from the AFM results of membranes prepared from 18 wt% PSf cast dope solutions precipitated in coagulation bath with different SDS concentration

SDS content (wt%)	Roughness parameters				Calculated pore parameters		
	R _a (nm)	R _q (nm)	R _z (nm)	Surface area ratio	Diameter (nm)	Geometric S.D. (σ _p)	Porosity (%)
0	4.3	3.4	44.6	1.08	27.3	1.40	13.3
0.15	4.4	3.5	31.2	1.04	31.0	1.48	14.9
0.25	4.8	4.0	31.0	1.03	24.8	1.69	18.3
0.3	3.6	2.9	24.7	1.03	26.4	1.49	16.8
0.4	3.8	3.1	25.4	1.04	39.3	1.46	16.7
0.5	4.5	3.5	27.9	1.05	42.4	1.50	13.8

became more detailed near the CMC value. The aperture of the pore-shaped structure of the membrane surface can be obtained by AFM data processing. Compared with the SEM, AFM in the test process does not need any treatment on the membrane surface, the test results can be a very true response to the surface morphology of the membrane. Thus, the aperture data of the pinhole structure on the membrane surface obtained from the AFM is more reliable. [40, 41]

The roughness data of the film measured by AFM and the calculated pore size and porosity are shown in Table 1. Below the CMC, the phase separation slowed down, the membrane cortex became thick and the surface porosity became smaller. Although the pores on the surface of the membrane are smaller, there is enough time to

induce the formation, resulting in the number of surface pores moves upward. The final morphology of membranes was determined by the two conflicting factors that the phase separation rate and time. When the concentration of SDS is below the CMC, as the concentration of SDS increases, the phase interface phase separation was hindered by SDS aggregated at the phase interface. The effect of pinhole diameter reduction on the porosity of the membrane is greater than the contribution of the pinhole number to the surface porosity. The surface roughness of the membrane gradually raises, but the surface of membranes and the overall surface area gradually decreased. Above CMC, micellar content and size also go up with increasing SDS concentration. In the range of 0.15% -

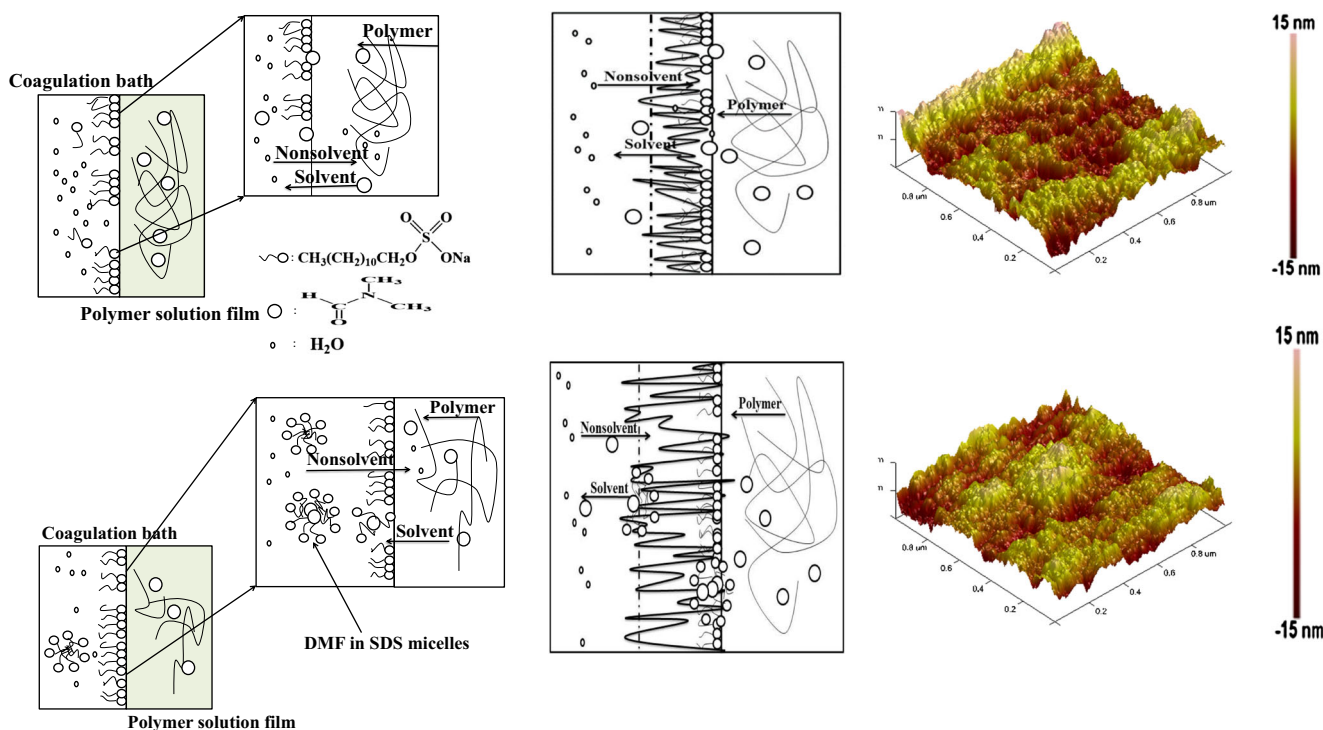


Fig. 6 Schematic drawing of the different diffusion rate on the formation of surface morphology

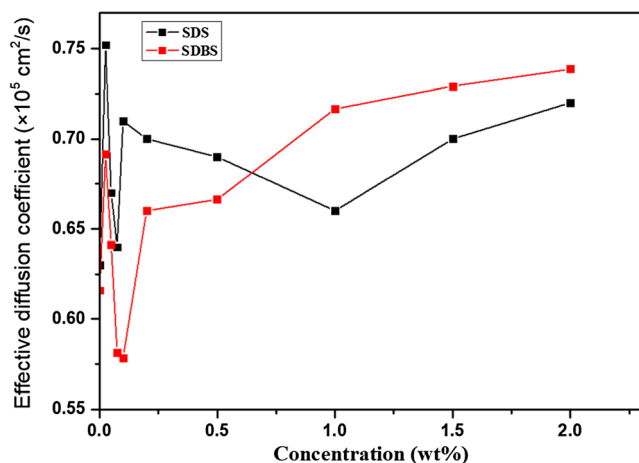


Fig. 7 Influence of SDS and SDBS concentration in 18 wt% PSf dope solutions on the phase separation rate

0.25 wt%, the number of micelles is gradually increased and the phase separation rate increases and the surface porosity moves upward. The influence of pinhole diameter ascends on the porosity of the membrane do more effect on the surface morphology than the contribution of the pinhole number to the surface porosity. Thus, the surface of membranes and surface area gradually decreased, thereby reducing the film surface roughness. The formation of membrane surface structure is more detailed. When the concentration of SDS exceeds 0.25%, the volume and number of micelles tend to be stable, and the phase separation rate is accelerated. As the micelles carry

DMF, the surface of the membrane will form larger pinholes and surface of membranes become more roughness. Therefore, as shown in Fig. 6, different diffusion rates form different surface structures.

SDS and SDBS were added to the casting solution

In order to reduce the concentration of SDS, further optimize the film preparation program. We attempted to add SDS to the casting solution. Experiments show that the preparation of 18 wt% PSf casting solution, which can add the SDS content of up to about 1 wt%. In order to verify the feasibility of the experiment, we chose another molecular structure with SDS similar to sodium dodecyl benzene sulfonate (SDBS) as a surfactant, for comparison.

Figure 7 is shown when different amounts of SDS and SDBS were added to the casting solution. When the pure water is used as the coagulation bath, the apparent diffusion coefficient of water diffusing into the casting solution tends to change with the surfactant. The phase separation rate tends to decrease first and then increase, which is similar to the addition of surfactant to the coagulation bath. As shown in Fig. 7, the addition of SDS to the casting solution increases the rate of phase separation at the beginning. When the additive is SDS, at the concentration of 0.05 wt% SDS, the phase separation rate tends to decrease first and then increase. The additive SDBS also has a similar phenomenon, but the critical value is 0.1 wt%. Initially, the casting solution of surfactant can also

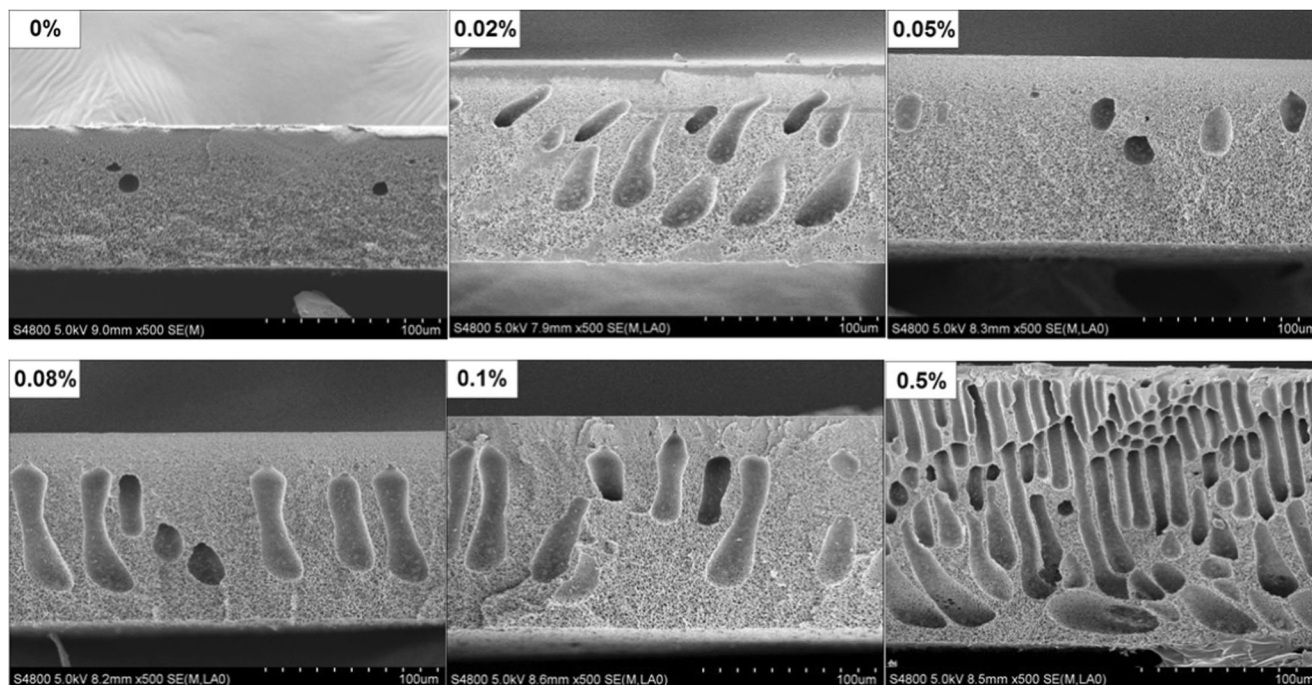


Fig. 8 SEM cross-section of membranes prepared from dope solutions having different SDS content

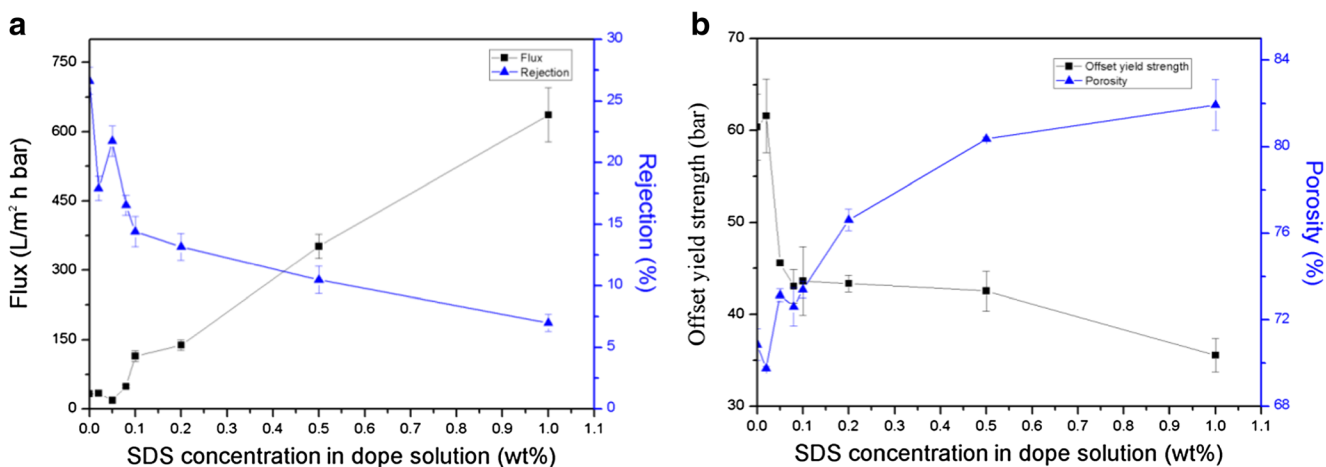


Fig. 9 Flux vs. rejection (a) and off-set yield strength vs. porosity (b) of membranes prepared with 18 wt% PSf dope solution having different SDS content

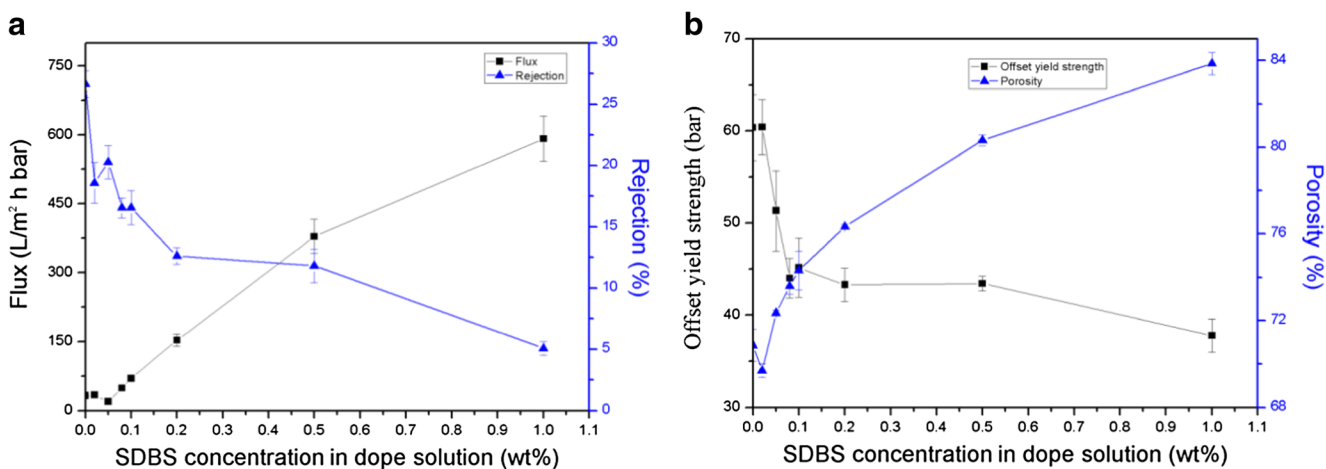


Fig. 10 Flux vs. rejection (a) and off-set yield strength vs. porosity (b) of membranes prepared with 18 wt% PSf dope solutions having different SDBS content

migrate to the membrane - bath interface, play a mechanical barrier role. When SDS formed micelles in the casting solution, the rate of phase separation began to go up, which is correspond to the phenomenon of surfactant added to the coagulation bath.

The SEM cross-section of membrane sections after addition of different contents of SDS is exhibited in Fig. 8. With the increase in SDS concentration, the trend of morphology of the membrane section changes as SDS was added to the casting

solution and the coagulation bath are similar. After adding 0.02 wt% SDS, the macrovoid structure of the membrane section increased significantly. When the SDS content increased to 0.05 wt%, the macrovoid structure of the membrane section was suppressed. Subsequently, the macrovoid structure becomes larger and runs through the entire membrane section. When the content exceeds than 0.5% wt, we can see that finger-like macropores ruins through the entire cross-section.

Table 2 Nature of the selected surfactants

Nomenclature	Chemistry name	HLB	Type	Character
Span-80	Sorbitan monooleate	4.3	Non-ion	Liquid
GMS	Glycerol monostearate	5.5	Non-ion	Solid
Tween-80	Polyoxyethylene sorbitan monostearate	15.0	Non-ion	Liquid
Tween-20	Polyoxyethylene sorbitan monolaurate	16.7	Non-ion	Liquid
SDBS	Sodium dodecyl benzene sulfonate	11.7	Ion	Solid
SDS	sodium dodecyl sulfate	40.0	Ion	Solid

Table 3 Viscosity of the dope solution having different surfactant content

Content (wt%)	Span-80 (mPa·s)	GMS (mPa·s)	Tween-80 (mPa·s)	Tween-20 (mPa·s)	SDBS (mPa·s)	SDS (mPa·s)
0.5	759.8	784.5	778.0	794.5	813.5	826.0
1.0	784.0	791.0	799.5	814.5	863.5	864.0

Table 4 Effective diffusion coefficient of the dope solution having different surfactant content

Content (wt%)	Span-80 (10^{-5} cm ² /s)	GMS (10^{-5} cm ² /s)	Tween-80 (10^{-5} cm ² /s)	Tween-20 (10^{-5} cm ² /s)	SDBS (10^{-5} cm ² /s)	SDS (10^{-5} cm ² /s)
0.5	0.64	0.63	0.71	0.67	0.71	0.70
1.0	0.72	0.66	0.80	0.71	0.71	0.65

After the addition of SDS and SDBS to the casting solution, the permeation performance and mechanical pressure resistance were changed illustrated in Fig. 9 and Fig. 10. This trend is similar to the addition of SDS in the coagulation bath. The addition of SDS to the casting solution can also achieve the purpose of improving the overall performance of the membrane. When the SDS in the casting solution is 0.08 wt% -0.1 wt%, the comprehensive performance of the membrane is better.

Effect of surfactant properties in casting solution

From the above studies, we have found that in the phase separation, the surfactant added to the casting solution will migrate into the coagulation bath as the exudation of solvent. If

we change the nature of the surfactant, it is bound to affect the phase separation of solvent and non-solvent exchange process, thereby changing the structure and performance of the membrane. Surfactants can express their affinity for water or oil according to their hydrophilic lipophilic balance (HLB), the greater the HLB value, the stronger hydrophilicity of the surfactant. In addition, depending on the form of dissociation of the surfactant in the solvent, it can be divided into ionic and nonionic. So we chose six surfactants, divided into two groups. One group is the ionic surfactant, SDS and SDBS, and the other is nonionic Span-80, GMS, Tween-80 and Tween-20. Their properties depicted in Table 2.

Table 3 shows the viscosity of the casting solution and the rate of phase separation observed under an optical microscope respectively after adding 0.5 wt% and 1 wt% of the surfactant.

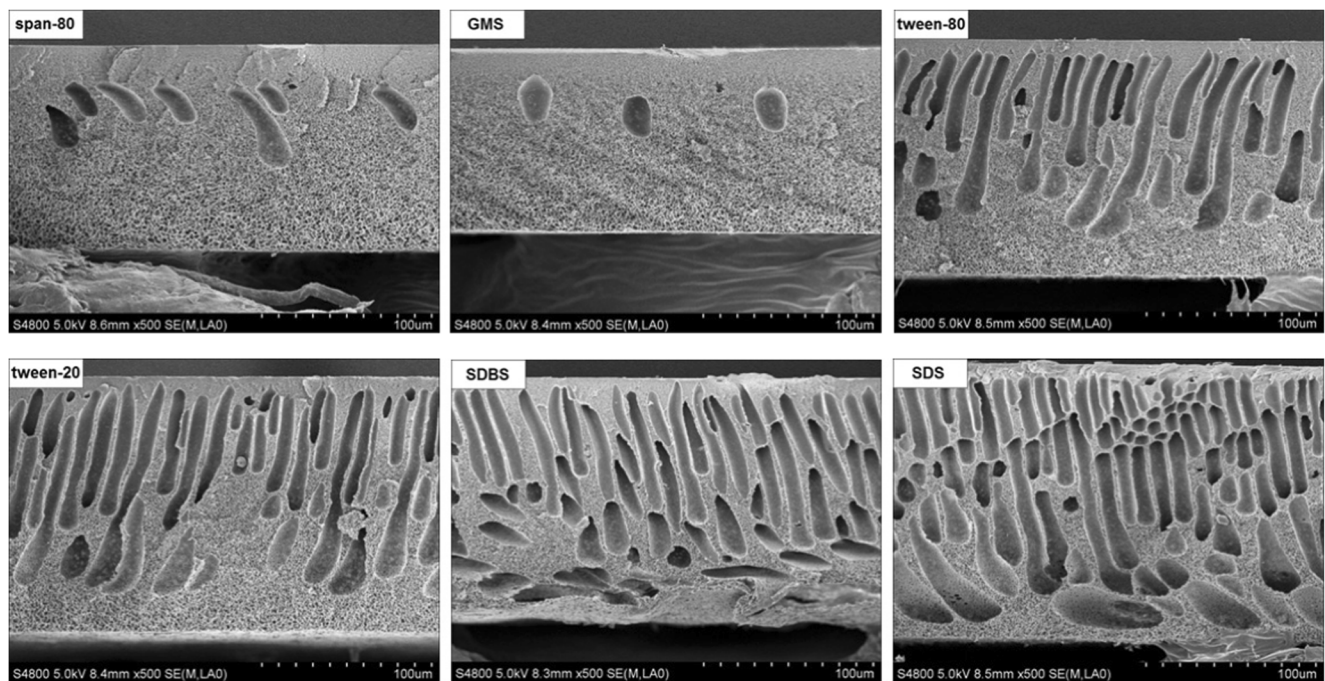


Fig. 11 SEM cross-section of membranes prepared from dope solutions having 0.5 wt% different surfactant

Table 5 Flux vs. rejection and yield stress vs. porosity properties of membranes prepared from dope solutions having different surfactant

Surfactant	Content (wt%)	Flux (L/m ² ·h·bar)	Rejection (%)	Off-set yield stress (Bar)	Porosity (%)
Span-80	0.5	28.1 ± 2.6	20.3 ± 0.8	56.4 ± 0.2	72.4 ± 0.8
	1.0	34.4 ± 2.6	15.2 ± 1.4	52.6 ± 2.7	72.9 ± 0.3
GMS	0.5	52.9 ± 4.1	16.9 ± 0.6	58.4 ± 2.9	70.5 ± 0.2
	1.0	61.7 ± 4.9	15.9 ± 1.4	62.5 ± 0.1	71.2 ± 0.2
Tween-80	0.5	98.0 ± 8.2	13.7 ± 1.1	54.4 ± 2.6	75.2 ± 0.6
	1.0	129.3 ± 15.5	12.3 ± 1.1	45.8 ± 3.9	77.9 ± 0.4
Tween-20	0.5	119.2 ± 15.2	18.2 ± 0.8	50.8 ± 4.4	77.5 ± 0.3
	1.0	306.4 ± 32.7	11.5 ± 0.8	41.1 ± 0.9	78.2 ± 0.2
SDBS	0.5	378.9 ± 37.0	11.8 ± 1.4	43.4 ± 0.8	80.3 ± 0.3
	1.0	592.0 ± 49.0	5.1 ± 0.6	37.8 ± 1.7	83.9 ± 0.5
SDS	0.5	352.1 ± 26.1	10.3 ± 1.1	42.5 ± 2.2	80.4 ± 0.1
	1.0	636.8 ± 59.2	7.0 ± 0.7	35.6 ± 1.8	81.9 ± 1.2

With the increase of surfactant HLB value, the viscosity of casting solution showed a general trend, the rate of phase separation also gradually accelerated as shown in Table 4. The greater the HLB value, the worse the compatibility of the surfactant with the casting solution, the more unstable the casting solution becomes, the higher of viscosity.

Figure 11 shows that SEM images of membrane sections after adding 0.5 wt% of different surfactants to the casting solution. With the increase of the HLB value of the surfactant, the macrovoid structure of the membrane showed an increasing trend. Table 5 for the prepared membrane permeability and pressure resistance, with the HLB value increases, the membrane flux is gradually increased, but the retention capacity of PEG20000 weakened. Considering all of the above surfactants, we found that when GMS was used as an additive for the casting solution, the overall performance of the prepared film was better.

Conclusion

In this paper, we choose the method of surfactant to change diffusion rate of the non-solvent into the polymer solution between membrane and coagulation bath. Whether the surfactant is added to the coagulation bath or the casting solution, the properties of the prepared film will inevitably change to a great extent. It was found that the addition of small amounts of surfactants in the coagulation bath or in the casting solution increases the surface of macrovoids and finger-like pores in the sub-layer of membranes. The surface analysis of membranes showed that mean pore size, pore density and surface porosity of membranes are higher at first compared to the membrane prepared without surfactant. As the SDS was added in the coagulation bath the surface of macrovoids and finger-like pores reached the minimum at 0.15 wt% SDS, then gradually increased. While the SDS in the casting solution is

0.08 wt% -0.1 wt%, the comprehensive performance of the membrane is better.

References

1. Ammar A, Elzatahry A, Al-Maadeed M, Alenzi AM, Huq AF, Karim A (2017) Nanoclay compatibilization of phase separated polysulfone/polyimide films for oxygen barrier. *Appl Clay Sci* 137:123–134
2. Lau WJ, Ismail AF, Misdan N, Kassim MA (2012) A recent progress in thin film composite membrane: a review. *Desalination* 287: 190–199
3. Mokhtari S, Rahimpour A, Shamsabadi AA, Habibzadeh S, Soroush M (2017) Enhancing performance and surface antifouling properties of polysulfone ultrafiltration membranes with salicylate-alumoxane nanoparticles. *Appl Surf Sci* 393:93–102
4. Veerababu P, Vyas BB, Singh PS, Ray P (2014) Limiting thickness of polyamide–polysulfone thin-film-composite nanofiltration membrane. *Desalination* 346:19–29
5. Buonomenna MG (2013) Membrane processes for a sustainable industrial growth. *RSC Adv* 3:5694
6. Strathmann H, Kock K (1977) The formation mechanism of phase inversion membranes. *Desalination* 21:241–255
7. Barth C, Gon Alves MC, Pires ATN, Roeder J, Wolf BA (2000) Asymmetric polysulfone and polyethersulfone membranes: effects of thermodynamic conditions during formation on their performance. *J Membr Sci* 169:287–299
8. Han G, Zhang S, Li X, Widjojo N, Chung T (2012) Thin film composite forward osmosis membranes based on polydopamine modified polysulfone substrates with enhancements in both water flux and salt rejection. *Chem Eng Sci* 80:219–231
9. Ghosh AK, Hoek EMV (2009) Impacts of support membrane structure and chemistry on polyamide–polysulfone interfacial composite membranes. *J Membr Sci* 336:140–148
10. Singh PS, Joshi SV, Trivedi JJ, Devmurari CV, Rao AP, Ghosh PK (2006) Probing the structural variations of thin film composite RO membranes obtained by coating polyamide over polysulfone membranes of different pore dimensions. *J Membr Sci* 278:19–25
11. Tiraferri A, Yip NY, Phillip WA, Schiffman JD, Elimelech M (2011) Relating performance of thin-film composite forward

- osmosis membranes to support layer formation and structure. *J Membr Sci* 367:340–352
12. Reuvers AJ, van den Berg JWA, Smolders CA (1987) Formation of membranes by means of immersion precipitation. *J Membr Sci* 34: 45–65
 13. Sadeghi I, Aroujalian A, Raisi A, Dabir B, Fathizadeh M (2013) Surface modification of polyethersulfone ultrafiltration membranes by corona air plasma for separation of oil/water emulsions. *J Membr Sci* 430:24–36
 14. Yu L, Yang F, Xiang M (2014) Phase separation in a PSf/DMF/water system: a proposed mechanism for macrovoid formation. *RSC Adv* 4:42391–42402
 15. Holda AK, Vankelecom IFJ (2014) Integrally skinned PSf-based SRNF-membranes prepared via phase inversion—part B: influence of low molecular weight additives. *J Membr Sci* 450:499–511
 16. Tsai H, Huang D, Ruaan R, Lai J (2001) Mechanical properties of asymmetric Polysulfone membranes containing surfactant as additives. *Ind Eng Chem Res* 40:5917–5922
 17. Saljoughi E, Sadrzadeh M, Mohammadi T (2009) Effect of preparation variables on morphology and pure water permeation flux through asymmetric cellulose acetate membranes. *J Membr Sci* 326:627–634
 18. Saljoughi E, Amirilargani M, Mohammadi T (2010) Effect of PEG additive and coagulation bath temperature on the morphology, permeability and thermal/chemical stability of asymmetric CA membranes. *Desalination* 262:72–78
 19. Struzyńska-Piron I, Bilad MR, Loccufier J, Vanmaele L, Vankelecom IFJ (2014) Influence of UV curing on morphology and performance of polysulfone membranes containing acrylates. *J Membr Sci* 462:17–27
 20. Tsai HA, Huang DH, Fan SC, Wang YC, Li CL, Lee KR, Lai JY (2002) Investigation of surfactant addition effect on the vapor permeation of aqueous ethanol mixtures through polysulfone hollow fiber membranes. *J Membr Sci* 198:245–258
 21. Boom R, Wienk I, Van den Boomgaard T, Smolders (1992) Microstructures in phase inversion membranes. Part 2. The role of a polymeric additive. *C. J Membr Sci* 73(2):277–292
 22. Cohen C, Tanny GB, Prager S Diffusion-controlled formation of porous structures in ternary polymer systems. *J Polym Sci Polym Phys Ed* 17:477–489
 23. Alsari AM, Khulbe KC, Matsuura T (2001) The effect of sodium dodecyl sulfate solutions as gelation media on the formation of PES membranes. *J Membr Sci* 188:279–293
 24. RAHIMPOUR A, MADAENI S, MANSOURPANAH Y (2007) The effect of anionic, non-ionic and cationic surfactants on morphology and performance of polyethersulfone ultrafiltration membranes for milk concentration. *J Membr Sci* 296:110–121
 25. Arena JT, McCloskey B, Freeman BD, McCutcheon JR (2011) Surface modification of thin film composite membrane support layers with polydopamine: enabling use of reverse osmosis membranes in pressure retarded osmosis. *J Membr Sci* 375:55–62
 26. Ching F, Lin, Wang DM, Lai CL, Yih J, Lai (1997) Effect of surfactants on the structure of PMMA membranes. *J Membrane Sci* 123:281–291
 27. Yih J, Lai, Ching F, Lin, Wu TT, Wang DM (1999) On the formation of macrovoids in PMMA membranes. *J Membrane Sci* 155: 31–43
 28. Jiang B, Wang BY, Zhang LH, Sun YL, Xiao XM, Yang N, Dou HZ (2017) Effect of Tween 80 on morphology and performance of poly(L-lactic acid) ultrafiltration membranes. *J Appl Polym Sci* 134
 29. Saedi S, Madaeni SS, Arabi Shamsabadi A, Mottaghi F (2012) The effect of surfactants on the structure and performance of PES membrane for separation of carbon dioxide from methane. *Sep Purif Technol* 99:104–119
 30. Tsai HA, Li LD, Lee KR, Wang YC, Li CL, Huang J, Lai JY (2000) Effect of surfactant addition on the morphology and pervaporation performance of asymmetric polysulfone membranes. *J Membrane Sci* 176:97–103
 31. Tsai H, Ruaan R, Wang D, Lai J (2002) Effect of temperature and span series surfactant on the structure of polysulfone membranes. *J Appl Polym Sci* 86:166–173
 32. Jeon MY, Yoo SH, Kim CK (2008) Effects of the support-layer hydrophilicity on the active-layer formation of composite membranes. *J Appl Polym Sci* 107:1194–1200
 33. Ramon GZ, Wong MCY, Hoek EMV (2012) Transport through composite membrane, part 1: is there an optimal support membrane? *J Membr Sci* 415–416:298–305
 34. Ruaan R, Chou H, Tsai H, Wang D, Lai J (2001) Factors affecting the nodule size of asymmetric PMMA membranes. *J Membr Sci* 190:135–145
 35. Dodda JM, Remiš T, Tomáš M, Novotný P (2015) Effect of alternation of polyamide selective layers in the formation and performance of thin-film composite membranes. *Desalin Water Treat* 57(19):8720–8729
 36. Liu X, Ng HY (2014) Double-blade casting technique for optimizing substrate membrane in thin-film composite forward osmosis membrane fabrication. *J Membr Sci* 469:112–126
 37. Ma N, Wei J, Qi S, Zhao Y, Gao Y, Tang CY (2013) Nanocomposite substrates for controlling internal concentration polarization in forward osmosis membranes. *J Membr Sci* 441:54–62
 38. Wang KY, Chung T, Amy G (2012) Developing thin-film-composite forward osmosis membranes on the PES/SPSf substrate through interfacial polymerization. *AICHE J* 58:770–781
 39. Matz R (1972) The structure of cellulose acetate membranes 1. The development of porous structures in anisotropic membranes. *Desalination* 10:1–15
 40. Rahimpour A, Madaeni SS (2007) Polyethersulfone (PES)/cellulose acetate phthalate (CAP) blend ultrafiltration membranes: preparation, morphology, performance and antifouling properties. *J Membr Sci* 305:299–312
 41. Singh S, Khulbe KC, Matsuura T, Ramamurthy P (1998) Membrane characterization by solute transport and atomic force microscopy. *J Membr Sci* 142:111–127